HHS Public Access

Author manuscript

Am J Transplant. Author manuscript; available in PMC 2023 June 01.

Published in final edited form as:

Am J Transplant. 2022 June ; 22(6): 1578–1592. doi:10.1111/ajt.17034.

IFI16-STING-NF-κB Signaling Controls Exogenous Mitochondrion-induced Endothelial Activation

Shu Li[1], **He Xu**[1,*], **Mingqing Song**[1], **Brian I Shaw**[1], **Qi-Jing Li**[2], **Allan D Kirk**[1,2]

[1]Duke Transplant Center, Department of Surgery, Duke University School of Medicine, Durham, NC, USA

[2]Department of Immunology, Duke University School of Medicine, Durham, NC, USA

Abstract

Mitochondria released from injured cells activate endothelial cells (ECs), fostering inflammatory processes, including allograft rejection. Stimulator of interferon genes (STING) senses endogenous mitochondrial DNA, triggering innate immune activation via NF-κB signaling. Here we show that exogenous mitochondria exposure induces EC STING-NF-κB activation, promoting EC/ effector memory T-cell adhesion, which is abrogated by NF-κB and STING inhibitors. STING activation in mitochondrion-activated ECs is independent of canonical cGMP-AMP synthetase sensing/signaling, but rather is mediated by interferon gamma–inducible factor 16 (IFI16) and can be inhibited by IFI16 inhibition. Internalized mitochondria undergo mitofusion and STING-dependent mitophagy, leading to selective sequestration of internalized mitochondria. Exposure of donor hearts to exogenous mitochondria activates murine heart ECs *in vivo*. Collectively, our results suggest that IFI16-STING-NF-κB signaling regulates exogenous mitochondrion-induced EC activation and mitophagy, and exogenous mitochondria foster T-cell–mediated CoBRR. These data suggest a novel, donor-directed, therapeutic approach toward mitigating perioperative allograft immunogenicity.

Keywords

Endothelial cells; mitochondria; stimulator of interferon genes; interferon gamma–inducible factor 16; NF-κB

INTRODUCTION

The immune response toward vascularized allografts is most intense in the early days posttransplantation. This heightened immunogenicity has been intuitively related to the immunostimulatory effects of injury inherent in organ procurement, storage and implantation, and empirically mitigated by heightened broad, “induction”

*To whom correspondence should be addressed: He Xu, MD, Departments of Surgery, Duke University School of Medicine, Edwin Jones Building Room 368, Durham, NC 27710, Phone: (919)684-4371, he.xu@duke.edu.

Conflict of interest: The authors have declared that no conflict of interest exists.

Competing interests: This submission is not published elsewhere and is not under consideration for publication elsewhere. It is the product of appropriate contributions by all authors’ and its authors are free of conflict-of-interest.

immunosuppression [1]. However, the mechanisms of early graft immunogenicity are incompletely understood, leaving the methods of preventing early allograft rejection (AR) imprecise [2].

Vascular endothelial cells (ECs) are the first physical barrier between a vascularized organ and host immunity, and likely play a critical role in initiating and regulating inflammatory reactions, such as AR [3–4]. In general, unstimulated ECs express low levels of adhesion, costimulatory and human leukocyte antigen (HLA) molecules. In contrast, activated ECs induced by conditions such as trauma [3–5], inflammatory disorders [3, 5–6], and AR [4, 6–7], upregulate adhesion, costimulatory, and HLA molecules, and produce leukocyte chemoattractants. These phenotypic changes are driven by many molecular effects of cell injury collectively termed “danger signals” [8], and play a crucial role in recruiting innate and adaptive immune cells, directing them to sites of EC activation [3–4, 6, 9–11]. Activated ECs serve as antigen presenting cells, providing costimulation to naïve T cells, and stimulating $CD28^-$ memory cells, which mediate anamnestic T-cell mediated immunoresponses [4–5, 7, 11–12]. These anamnestic immunoresponses are believed to be important in mediating costimulation blockade–resistant rejection (CoBRR), a process that is therapeutically relevant in organ transplantation [13–14].

Damage-associated molecular patterns (DAMPs) are molecules and microparticles released during major trauma [15], surgical procedures [16], and brain injuries [17]. Extracellular mitochondria and mitochondria DNA (mtDNA) released from damaged mitochondria are a major source of DAMPs, activate ECs, and play an important role in inducing inflammation [18–20] and initiating immunoresponses [21–22], including AR [23–24]. Indeed, mtDNA is known to be present in brain dead organ donors and has been shown to augment subsequent alloimmune responsiveness to organs derived from those donors [24].

It is believed that EC activation forms a mechanistic centerpiece of DAMP signaling, and DAMP presence proportionately augments inflammation and organ immunogenicity [3–4, 7–8]. Recently, we and our collaborators have demonstrated a direct interaction between exogenous mitochondria and ECs leading to contact-dependent EC activation, and CoBRR in a MHC-mismatched murine heart transplant model [24]. However, the mechanisms governing this process have not been explicitly investigated.

The nuclear factor kappa-B (NF-κB) transcriptional complex plays a key role in controlling inflammatory and immunoresponses of cells, including ECs, to a variety of stimuli [25–26]. Recent studies have demonstrated that the stimulator of interferon genes (STING), an intracellular sensor of pathogen-derived and endogenous DNA [27–28], initiates NF-κB-mediated innate immunoresponses by cytosolic/canonical [29] or nuclear/non-canonical [30] pathways. In this study, we investigate the role of cyclic GMP-AMP synthetase (cGAS), a cytosolic signaling molecule, and interferon gamma–inducible factor-16 (IFI16), a nuclear signaling molecule, in activating STING in human ECs following interaction with exogenous mitochondria. We find that mitochondrion–induced EC activation is driven by non-canonical STING activation, can be dampened by inhibition of IFI16, fosters EC interactions with T cells, and stimulates mitophagy of internalized mitochondria. We further show that exposure of donor hearts to exogenous mitochondria activates graft EC

and promotes memory T-cell–mediated B7-CoBRR of MHC-mismatched mouse cardiac allografts.

Methods

Extrinsic mitochondrial-inducted endothelial activation

For EC activation experiments, purified mitochondria were added into plates containing ECs. In selected experiments, mitochondria were placed into a transwell-insert (0.4 μm pore) with confluent ECs. ECs were stained with mAbs after mitochondrion–stimulation. The viability/apoptosis of ECs was assessed using a viability kit, and intracellularly stained anti-active-caspase-3 mAb to verify cell death/apoptosis (Fig. S1).

To measure intracellular cytokines, ECs were incubated with 100 μg/mL mitochondria for 12-hours with GolgiPlug™. Cells were stained with anti-IL-6, IL-8, and MCP-1 mAbs after fixation/permeabilization, and analyzed by florescence activated cell sorting (FACS). The culture supernatants without GolgiPlug™ were measured to verify IL-6 production (Fig. S2). To determine the uptake of mitochondria by ECs, dsRed-expressing mitochondria were incubated with ECs followed by FACS and analyzed using FlowJo software (Tree Star).

Detection of phosphorylation of intracellular targets in mitochondrion–stimulated endothelial cells.

The NF-κB-p65 activity of ECs during mitochondrion–EC interaction was assessed by detection of NF-κB-p65 phosphorylation at serine residue-529 that occurs during the NF-κB-p65 activation. ECs were collected from mitochondrion–EC coculture, and fixed with Cytofix followed by permeabilization with prechilled-Perm-Buffer-III. Cells were stained with anti-NF-κB-p65(pS529) mAb followed by FACS analysis.

To detect the activation of STING as determined by the phosphorylation site Ser366 in ECs, the mitochondrion-stimulated ECs were fixed with Cytofix and permeabilized with prechilled-Perm-Buffer-III followed by staining with anti-STING-ser366 mAbs. Cells were stained with Alexa-Fluor-488 secondary antibody and analyzed by FACS.

Inhibition of mitochondrion–induced endothelial cell activation.

To determine the role of NF-κB in regulating mitochondrion–induced EC activation, ECs were treated 10 μM NF-κB inhibitor Bay11–7082 and vehicle solution followed by stimulation with 50 μg/mL mitochondria. Cells were stained with anti-CD54 and CD106 mAbs.

To assess the role of STING-IFI16 signaling in regulating mitochondrion–induced EC activation, ECs were treated with STING inhibitor H151 or vehicle solution. In selected experiments in evaluating upstream signaling of STING, ECs were treated with IFI16 inhibitor ODN TTAGGG (A151) or ODN control, and cGAS inhibitor RU.521. Cells were stained with anti-CD54 and CD106 mAbs.

To determine the role of toll-like receptor-9 (TLR9)/MyD88 in mitochondrion–induced EC activation, ECs were treated with DRQIKIWFQNRRMKWKKRDVLPGT (MyD88

homodimerization sequence: RDVLPGT) and DRQIKIWFQNRRMKWKK (control) and incubated with mitochondria followed by surface-staining for CD54 and CD106.

Measurement of 2′3′cGAMP by enzyme-linked immunosorbent assay (ELISA)

The 2′3′cGAMP was measured by the 2′3′cGAMP ELISA kit according to protocol. Briefly, ECs were stimulated with 50 μg/mL mitochondria, and incubated with protein extraction reagent. The samples were added to pre-coated-ELISA-plate under competition with 2′3′cGAMP-HRP tracers. The 2′3′cGAMP concentration was determined by measuring the HRP enzymatic activity using the chromogenic substrate 3,3’,5,5’-tetramethylbenzidine. The reaction was measured at 450 nm. The intensity of color was proportional to the amount of 2’3’cGAMP-HRP tracer which was inversely proportional to the amount of 2’3’cGAMP in the samples.

Image-based FACS, live-cell video-microscopy, and florescent imaging

To assess the interaction between internalized exogenous mitochondria and ECs, EC endogenous mitochondria were pre-labeled with MitoTracker-Green, and EC lysosomes were labeled with LysoTracker-Blue. ECs were incubated with dsRed-expressing mitochondria followed by ImageStream®^{X} Mark-II-Imaging-FACS to measure colocalization of exogenous mitochondria with endogenous mitochondria or lysosome.

Live-EC imaging was performed on a Zeiss-Axiovert-100TV station (Roper Scientific). Endogenous EC mitochondria were pre-labeled with MitoTracker-Green and incubated with dsRed-expressing mitochondria. The cultures were placed on the imaging-station to record the dynamics of mitochondrial fusion for 4 hours with 3-D optical section of 0.5 μm increments and 10 μm depth. The imaging was analyzed using AutoQuant (Media Cybernetics) and MetaMorph (Molecular Devices).

To investigate the role of IFI16 during EC–mitochondrion interaction, ECs were stimulated by mitochondria for 60 and 120 minutes. ECs were fixed with 2% formaldehyde and incubated with anti-IFI16 or isotype-Ig followed by incubation with goat anti-mouse IgG-DyLight-488. Cells were evaluated by Zeiss-LSM780 microscope.

To evaluate the autophagy/mitophagy, FACS was performed to measure autophagic vacuoles following EC–mitochondrion coculture using the Autophagy-Green-Dye with or without autophagy inhibitor 3-methyladenine (3-MA). In selected experiments, ECs were treated with STING inhibitor H151 and stained with Autophagy-Green-Dye. Microscopic florescent image was utilized to analyze the mitophagy during exogenous mitochondrion–EC interaction. Briefly, ECs were cocultured with dsRed-expressing mitochondria and fixed with pre-chilled-methanol followed by permeabilization with Triton-X-100. Cells were stained with anti-LC3B antibody, and incubated with goat anti-rabbit IgG-Alexa-Fluor-488. The image was analyzed with Zeiss-LSM780 microscope.

Infusion of mitochondria and immunological analysis

200 μg mouse mitochondria were infused into BALB/c mice via tail vein. Hearts were collected at various time points post-infusion, and frozen sections of tissue were stained

with anti-CD54 and MHC-class-I mAbs. The expression of CD54 and MHC-class-I was semi-quantified by Aprio ImageScope Software (Leica Biosystems).

Statistical analysis

Unpaired Student's two-tailed *t*-test was performed to determine the statistical significance between mitochondrion–treated ECs and control ECs. A log-rank (Mantel-Cox) test was utilized to evaluate statistical significance of allograft survival. A *p*-value of less than 0.05 was considered statistically significant.

Results

Exogenous mitochondria activate endothelial cells, augmenting adhesion to memory T cells.

Primary ECs were incubated with purified mitochondria at different concentrations for 12 hours followed by FACS analysis to verify the capacity of mitochondria to induce EC activation. Mitochondrion exposure led to dose-, contact- and time-dependent upregulation of CD54, CD62E and CD106 (Fig. S3), confirming and expanding on previous observations [24]. Additionally, IL-6, IL-8, and MCP-1 production, all critical in recruiting immune cells [3–4], was increased during EC exposure to mitochondria (Fig. 1a).

To evaluate the effects of extracellular mitochondria on EC activation *in vivo*, mouse mitochondria were infused intravenously into BALB/c mice. Hearts were collected at multiple time points post-infusion. Immunohistological analysis of hearts showed significant, prompt, but transient upregulation of CD54 and MHC-Class-I expression on the endomyocardial EC surface at 8 hours post-infusion, which waned by 24 hours (Fig. 1b).

To assess the impact of mitochondrial exposure on the ability of ECs to augment T-cell adhesion, an allogeneic T-cell–EC adhesion model was established using untreated ECs, or EC preconditioned with extrinsic mitochondria or tumor necrosis factor alpha (TNF-α), in coculture with allogeneic PBMCs. The adherent PBMCs were phenotypically characterized by FACS. As shown in Fig. 1c, prior mitochondrial or TNF-α exposure significantly increased $CD3^+$ T-cell adhesion to ECs. The adherent T cells were predominantly $CD8^+$. Based on CD197/CD45RA classification [31–32], the adherent T cells were effector memory cells ($T_{EM,}$ $CD45RA^-CD197^-$) and terminally differential effector memory cells ($T_{EMRA,}$ $CD45RA^+CD197^-$), subsets known to have reduced costimulation requirements and to be involved in CoBRR [14, 32]. The adhesion of naïve ($T_{Naïve,}$ $CD45RA^+CD197^+$) and central memory cells ($T_{CM,}$ $CD45RA^-CD197^+$) was comparatively low (Fig. 1c). Furthermore, the majority of adherent $CD8^+$ cells lacked CD28 expression and highly expressed CD11a (Fig. 1d), important surface molecules providing CD80/86 costimulation- and CD54-dependent adhesion, respectively [11]. Proliferating T cells in response to allogeneic EC exposure expressed significantly higher levels of CD11a (Fig S4).

Exogenous mitochondria induce endothelial NF-κB signaling.

NF-κB signaling plays a critical role in regulating EC activation and the production of inflammatory mediators [33–34]. To determine the major intracellular signaling

mechanisms controlling mitochondrion-induced EC activation, we first measured the NF-κB phosphorylation during mitochondrion–EC interactions. As shown in Fig. 2a, ECs exhibited a significant increase of NF-κB-p65 subunit phosphorylation at serine 529 within 30 minutes of initial mitochondrion–stimulation. IκB-α/NF-κB inhibitor Bay11–7082 prevented EC upregulation of CD54 and CD106 induced by exogenous mitochondria (Fig. 2b), suggesting that mitochondrion–induced EC activation is mediated through the NF-κB signaling.

STING activation controls exogenous mitochondrion-mediated endothelial activation.

STING is both a DNA sensor molecule and an adaptor protein localized on the endoplasmic reticulum (ER) particularly at contact points between the ER and mitochondria [35]. It is activated by interaction with cyclic GMP-AMP, which is generated by cGAS following its sensing of pathogen-derived cytosolic DNA [27–28]. Activated STING, in turn, initiates NF-κB-mediated innate immunoresponses [29–30]. Previous studies have implicated STING signaling in EC activation in tumors, leading to lymphocyte migration and cell-mediated immunoresponses [36–37]. We therefore sought to determine whether the STING activation played a role in regulating EC activation following exogenous mitochondrion–stimulation. First, ECs rapidly phosphorylated STING at Ser366 after coculture with exogenous mitochondria (Fig. 3a). Further, when ECs were treated with STING inhibitor H151 [38], their activation following mitochondrion–stimulation was markedly inhibited (Fig. 3b).

Canonical STING activation is induced by the binding of the second messenger cyclic GMP-AMP (2′3′cGAMP), generated by cGAS, a cytosolic DNA sensor that binds directly to damaged DNA [27–28]. To evaluate the role of this pathway in initiating EC activation, the production of intracellular 2′3′cGAMP was measured in ECs following mitochondrion–stimulation. ECs pretreated with RU.521, a cGAS inhibitor [39], were analyzed by measuring CD54 and CD106 expression prior to mitochondrion–stimulation. As shown in Fig. 3c, mitochondrion–stimulation did not increase 2′3′cGAMP production. Furthermore, cGAS inhibition did not prevent EC activation following their interaction with mitochondria (Fig. 3d). Thus, cGAS-cGAMP-STING signaling did not appear to participate in mitochondrion-induced EC activation.

IFI16 plays a key role in exogenous mitochondrion-induced endothelial activation

STING can also be triggered in a non-canonical pathway via the binding of damaged DNA to IFI16 [30]. IFI16, a nuclear inflammasome receptor that recognizes pathogen–associated molecular patterns, interacts with STING leading to induction of IFN-β responses [40]. To assess the role of this alternative pathway to STING activation, we first verified the IFI16 expression in ECs by intracellular staining. Intracellular IFI16 expression was confirmed in unstimulated ECs, and increased slightly following IFN-γ-stimulation (Fig. S5a). Confocal florescent imaging demonstrated that IFI16 protein was localized within the endothelial nucleus (Fig. S5b).

To assess the role of IFI16 during exogenous mitochondrion–EC interactions, ECs were co-incubated with purified mitochondria followed by FACS and confocal florescent imaging. As shown in Fig. 4a–b, mitochondrion exposure significantly increased EC expression of

IFI16. Florescent imaging analysis showed a significant increase in nuclear DNA covered by IFI16, and an increase in free IFI16 (Fig. 4c), suggesting that IFI16 reached a saturation point for intra-nuclear DNA coverage and was in excess of the available binding sites.

To further evaluate the role of IFI16 in inducing STING-dependent, mitochondrion-induced EC activation, we treated ECs with A151, a synthetic oligodeoxynucleotide that blocks both IFI16 and toll-like-receptor-9 (TLR9) [41–42] and performed coincubation with mitochondria. As shown in Fig. 4d, pretreatment of ECs by A151, but not an ODN control, prevented EC activation.

Since A151 inhibits both IFI16 and TLR9, we next sought to determine whether TLR9 inhibition could alter mitochondrion–induced EC activation. Previous studies have detected the presence of TLR9 in human lymphatic ECs [43], a finding we replicated (Fig. S6a). Moreover, TLR9 binds to bacterial DNA CpG-motifs leading to cell-activation via MyD88-NF-κB-dependent signaling [44–45]. Therefore, we investigated the effect of TLR9-MyD88 signaling in ECs following mitochondrion-stimulation by pretreating ECs with MyD88 inhibitor pepinh-MYD. As shown in Fig. S6b, pepinh-MYD did not prevent mitochondrion–induced EC activation, but NF-κB inhibition with Bay11–7082 did, indicating that the NF-κB-dependent EC activation by mitochondria is independent of TLR9-MyD88 signaling.

Internalized extrinsic mitochondria undergo mitofusion and STING-dependent mitophagy.

ECs internalize apoptotic cells, bacteria, microparticles and free mitochondria via scavenger receptors [24, 46–47]. Given the inflammatory nature of exogenous, and presumably stressed mitochondria, we sought to determine whether mitochondrion–induced IFI16-STING activation influenced sequestration of mitochondria by induction of mitophagy. Using an Image-Stream-FACS, we semi-quantitatively examined the internalization of exogenous mitochondria by ECs following 4-hour coincubation, and using a live-3-D imaging system, demonstrated active fusion of green-florescent-labeled endogenous mitochondria with dsRed-labeled exogenous mitochondria, and its accompanying increase in ATP production (Fig. S7).

Subsequent FACS analysis showed increased mitophagy during mitochondrion–EC coincubation (Fig. 5a), that was reduced through the inhibition of type-III phosphatidylinositol 3-kinases by 3-MA (Fig. 5b). To further define the mitochondria targeted for removal, EC lysosomes were pre-labeled with LysoTracker-Blue and native EC mitochondria were pre-labeled with green-florescent-MitoTracker, followed by coincubation with dsRed-transfected mitochondria. There was minimal mitophagy of native mitochondria (Fig. 5c). In contrast, there was a significant increase in colocalization of internalized mitochondria with lysosomes in EC–mitochondria cocultures (Fig. 5c), indicating selective mitophagy of internalized mitochondria. Indeed, after internalization of dsRed-expressing mitochondria, ECs assembled autophagosomes with exogenous mitochondria, localizing mitochondria with microtubule-associated protein-1 light chain-3 (LC3) (Fig. 5d), which mediates membrane expansion and fusion with lysosomes for degradation. As such, uptake and processing of exogenous mitochondria was observed to be an active and specific event.

Recent studies have shown that STING activation triggers autophagy by a direct interaction of activated STING with LC3 interacting region (LIR) motifs of LC3 [48] or participating as a membrane source for LC3 lipidation [49]. Furthermore, activation of PTEN-induced kinse1 (PINK1) recruits parkin to damaged mitochondria, triggering autophagy [50], and mitigate the inflammation induced by STING signaling [51]. To determine whether STING activation could trigger mitophagy in mitochondrion–stimulated ECs, ECs were pre-treated with H151 prior to mitochondrion exposure, and mitochondrion–induced EC mitophagy was measured by staining with the fluorescent probe monodansylcadaverine, which is specific for lysosomal/autophagic vacuoles. As shown in Fig. 5e, mitophagy was significantly prevented in H151-treated ECs, suggesting that STING activation promotes mitophagy in ECs following their interaction with mitochondria.

Discussion

It has been empirically determined that organ allografts require substantially augmented immunosuppression, so called induction immunosuppression, to prevent rejection early posttransplantation [1]. The need for induction has been attributed to increased immunogenicity, variably related to the hyperinflammatory state in the donor, and injury associated with organ preservation/ischemia/reperfusion. Common to all these states are the liberation of DAMPs, including mitochondrial contents from cell death in the donor (particularly terminal brain injury) and the graft itself [52], and concomitant endothelial activation manifest by increased adhesion molecule expression and chemotactic cytokine liberation [3–6]. Herein, we have specifically examined the role of liberated mitochondria on endothelial activation, and further defined the intracellular pathways specifically responsible for the long-recognized, generic immunogenicity of a newly transplanted organ. We find that STING-NF-kB sensor pathways are active in orchestrating the response to free mitochondria, and that this response is relevant to the processes leading to memory T cell-mediated CoBRR [24].

Common to essentially all clinical induction immunosuppressive protocols are high dose glucocorticosteroids, which are known to exert broad anti-inflammatory effects through inhibition of NF-kB [53]. In this study, we expose a central role of NF-kB in the response of ECs to exogenous mitochondria. Specifically, we find increased phosphorylation of the NF-κB-p65 subunit in ECs following interactions with mitochondria, and show that NF-κB inhibitor completely abrogates mitochondrial-induced EC activation. This finding highlights a potential means by which steroid induction limits early EC-driven inflammation [53].

Several intracellular signaling pathways directly involve NF-κB regulated cell activation [25–30, 45, 54]. In our studies, EC activation could not be prevented by MyD88 inhibition, indicating that mitochondrion–stimulation is independent of TLR9-MyD88-NF-κB signaling [45, 55]. It has been well-documented that STING, a protein localized to the ER that serves as an adaptor protein in sensing intracellular pathogens, triggers NF-κB-mediated innate immunoresponses via type-I interferon production [27–29]. ECs express STING and STING activation has been shown to propagate T cell-mediated antitumor immunity [36–37]. Herein, we find for the first time that ECs demonstrate STING phosphorylation after exposure to exogenous mitochondria, and the inhibition of STING activity with STING-

specific inhibitor effectively prevents EC activation. Thus, STING-NF-κB signaling plays a role in regulating DAMP-mediated EC activation.

STING signaling is a downstream target for cGAS-cGAMP [28], a cytosolic signal, and IFI16 [30, 40], a non-canonical, nuclear signal. In this study, ECs did not produce 2′3′cGAMP following exogenous mitochondrial exposure, and EC activation was not prevented by the inhibition of cGAS, suggesting that the STING activation in this context is independent of cGAS-cGAMP signaling.

Unlike cytosolic signaling via cGAS-cGAMP sensing danger elements, IFI16 detects damaged DNA, and induces rapid activation of the STING-NF-κB signaling [30, 40]. Unlike the effects with cGAS inhibition, we have shown that ECs upregulate IFI16 during their interaction with exogenous mitochondria. The IFI16 disassociates with nuclear DNA, and translocates to cover the surface of nuclear DNA, where IFI16 senses internalized mitochondria, and directly interacts with STING residing in the ER to trigger STING activation [30, 40]. Indeed, the inhibition of IFI16 by ODN-TTAGGG effectively prevented mitochondria-induced EC activation. These findings indicate IFI16 detects exogenous mitochondria and regulates STING activity, making IFI16-STING-NF-κB signaling critical in regulating DAMP-induced EC activation. Notably, STING phosphorylation occurs in ECs following exogenous mitochondrion–stimulation but not in the cells with intracellular damaged DNA-induced STING activation [40], suggesting distinct mechanisms in regulating STING activation by IFI16. The mechanisms by which IFI16 recognizes exogenous mitochondria remains to be established.

This study confirms our recent finding of class-A scavenger receptor-mediated internalization of exogenous mitochondria by human ECs [24], which is also consistent with other previous reports [46–47]. Mitochondria influence cell apoptosis in part through the regulation of Bcl-2 family members in coordination with caspase activation and release of cytochrome-c [56]. Thus, internalization of exogenous mitochondria released from damaged-cells may induce ECs to undergo apoptosis. Counter-intuitively, in this setting, internalized mitochondria were insufficient to induce EC apoptosis attributed by several mechanisms. First, mitochondrion–fusion between internalized mitochondria and endogenous mitochondrial [24] with increasing ATP production [57] may stabilize the endothelium, preserving the health of cells, as has been suggested [58–59]. Second, a large fraction of internalized mitochondria assembles with autophagosomes, and lysosomes in undergoing mitophagy, a mechanism in preventing cell damage induced by abnormal intracellular organelles [60]. Third, a most important finding, we show that STING signaling plays a critical in regulating mitophagy in ECs following internalization of exogenous mitochondria. We speculate that interaction between activated STING and LC3 [48–49] may initiate this process in ECs. Altogether, our findings represent a fundamental process for the important role of mitochondrion–fusion and mitophagy in controlling deleterious consequences to healthy ECs exposed to exogenous mitochondria.

We have explored the links between the cellular events detailed above and the broader phenotype of organ rejection. As we previously reported, the interaction of exogenous mitochondria with ECs results in upregulated CD54 and CD106 [24], both critical in

initiating immune cell adhesion and activation [10–11]. Indeed, recipients receiving heart allografts from donors that are preconditioned with exogenous mitochondrion infusion, demonstrate CoBRR in the presence of B7 inhibitor [24]. In this study we find the effects of EC activation disproportionately influences T_{EM}/T_{EMRA} subsets. This is particularly relevant when considering B7-CoB as a therapeutic option for allotransplantation, as in humans these subsets frequently lack the CD28 and are known to participate in memory cell-mediated CoBRR [14, 32, 61]. Thus, this exogenous mitochondria-induced EC activation may play a disproportionate role in augmenting rejection when immunosuppression relies on CoB, and explain why CoBRR can be controlled by intense depletional induction therapy [62], and becomes decreasingly problematic with increasing time posttransplantation [63].

We extended these *in vitro* observations to show that mitochondrial infusion results in upregulation of CD54 and MHC class I expression on hearts *in vivo*. Mitochondria are known to be released from damaged cells during trauma [16, 18, 21], and inflammatory changes and accumulation of DAMPs [64–67] have been observed in deceased donors. Our studies show that circulating DAMPs can directly induce EC activation, and suggest that the exposure of donor allografts to exogenous mitochondria prior to transplantation may promote CoBRR in mouse recipients undergoing B7-CoB monotherapy. These results demonstrate a potential role for mitochondria-EC interactions in leading to CoBRR.

Given the relationship between DAMPs and donor allografts, these findings highlight a novel and potentially tractable risk factor for CoB resistance that provides both a means of risk stratification and a potential therapeutic target in patients being considered for CoB–based regimens.

In conclusion, our observations demonstrate mechanisms by which exogenous mitochondria induce human EC activation and subsequently augmenting T-cell activity, impairing the efficacy of B7-CoB immunosuppressive strategies in vascularized allotransplantation. Specifically, we demonstrate that IFI16-STING-NF-κB signaling plays a critical role in regulating human EC activation in response to exogenous mitochondrial stimulation. Activated-STING plays a key role in triggering mitophagy in ECs following interaction with exogenous mitochondria. We also show that mitochondrion–induced EC activation is independent of cGAS-cGAMP-STING and TLR-9-MyD88 signaling pathways. Of note, internalized mitochondria undergo mitofusion and mitophagy with increased anti-apoptotic activity, the major mechanisms in preserving the health of endothelium. Thus, we propose that exogenous mitochondria directly activate EC in an IFI16-STING-NF-κB-dependent signaling, and the activation of ECs triggers T cell–mediated CoBRR.

Supplementary Material

Refer to Web version on PubMed Central for supplementary material.

Acknowledgments

The authors gratefully acknowledge Drs. Jun Wang and Linda Cendales for their expert technical assistance in mouse cardiac transplantation, MacKenzie MaRae, BA, for her assistance in establishing mitochondrial purification protocol, and Elizabeth Wong, PhD, for her work in transducing florescent protein dsRed targeted to mitochondria in HeLa cells.

Funding information:

This work was funded in part by grants from the Roche Organ Transplant Research Foundation grant (346678023, HX) and the National Institutes of Health (AI097423, ADK).

Data availability:

The datasets produced and analysed during the current study are available in the Duke Surgery repository (\\duhsnas-pri\dusom_surg_kirk_lab). All datasets generated during and/or analysed during this study are included in the published article (and its supplementary information files). The datasets generated during and/or analysed during the current study are currently not publicly available as unpublished data but are available from the corresponding author on reasonable request.

Abbreviations

ECs	Endothelial cells
FACS	Florescence activated cell sorting
NF-κB	Nuclear factor-kappa B
STING	Stimulator of interferon genes
IFI16	Interferon gamma–inducible factor 16
CoBRR	Costimulation blockade–resistant rejection
AR	Allograft rejection
HLA	Human leukocyte antigen
DAMPs	Damage-associated molecular patterns
mtDNA	Mitochondria DNA
cGAS	Cyclic GMP-AMP synthetase
mAbs	Monoclonal antibodies
FACS	Florescence activated cell sorting
ELISA	Enzyme-linked immunosorbent assay
PBMCs	Peripheral blood mononuclear cells
TNF-α	Tumor necrosis factor alpha
TLR9	Toll-like receptor 9
ER	Endoplasmic reticulum

Reference

1. Kirk A Induction immunosuppression. Transplantation. 82, 593–602 (2006). [PubMed: 16969280]

2. Rosenblum JM, Kirk A. Recollective homeostasis and the immune consequences of peritransplant depletional induction therapy. Immunol Rev. 258, 167–182 (2014). [PubMed: 24517433]
3. Pober JS, Sessa WC. Evolving function of endothelial cells in inflammation. Nat Rev Immunol. 7, 803–815 (2007). [PubMed: 17893694]
4. Briscoe DM, Alexander SI, Lichtman AH. Interactions between T lymphocytes and endothelial cells in allograft rejection. Curr Opin Immunol. 10, 525–531 (1998). [PubMed: 9794840]
5. Henn V, Slupsky JR, Grafe M, et al. CD40 ligand on activated platelets triggers an inflammatory reaction of endothelial cells. Nature. 391, 591–59 (1998). [PubMed: 9468137]
6. Walker JD, Maier CL, Pober JS. Cytomegalovirus-infected human endothelial cells can stimulate allogeneic CD4+ memory T cells by releasing antigenic exosomes. J Immunol. 182, 1548–1559 (2009). [PubMed: 19155503]
7. Kirk AD, Morrell CN, Baldwin WM 3rd. Platelets influence vascularized organ transplants from start to finish. Am J Transplant. 9, 14–22 (2009). [PubMed: 19067663]
8. Matzinger P The danger model: a renewed sense of self. Science. 296, 301–305 (2002). [PubMed: 11951032]
9. Hancock WW, Sayegh MH, Zheng XG, Peach R, Linsley PS, Turka LA. Costimulatory function and expression of CD40 ligand, CD80, and CD86 in vascularized murine cardiac allograft rejection. Proc Natl Acad Sci USA. 93, 13967–13972 (1996). [PubMed: 8943044]
10. Damle NK, Aruffo A. Vascular cell adhesion molecule 1 induces T-cell antigen receptor-dependent activation of CD4+ T lymphocytes. Proc Natl Acad Sci USA. 88, 6403–6407 (1991). [PubMed: 1713678]
11. Sancho D, Yanex-Mo M, Tejedor R, Sanchez-Madrid F. Activation of peripheral blood T cells by interaction and migration through endothelium: role of lymphocyte function antigen-1/intercellular adhesion molecule-1 and interleukin-15. Blood. 93, 886–896 (1999). [PubMed: 9920837]
12. Denton MD, Geehan CS, Alexander SI, Sayegh MH, Briscoe. Endothelial cells modify the costimulatory capacity of transmigrating leukocytes and promote CD28- mediated CD4(+) T cell alloactivation. J Exp Med. 190, 555–566 (1999). [PubMed: 10449526]
13. Vincenti F, Larsen CP, Alberu J, et al. Three-year outcomes form BENEFIT, a randomized active-controlled, parallel-group study in adult kidney transplant recipient. Am J Transplant. 12, 210–217 (2012). [PubMed: 21992533]
14. Espinosa J, Herr F, Tharp G, Bosinger S, Song M, Farris AB 3rd., George R, Cheeseman J, Stempora L, Townsend R, Durrbach A, an Kirk AD. CD57+ CD4 T cells underlie belatacept-resistant allograft rejection. Am J Transplant. 16, 1102–1112 (2016). [PubMed: 26603381]
15. Simmons JD, Lee YL, Mulekar S, et al. Elevated levels of plasma mitochondrial DNA DAMPs are linked to clinical outcome in severely injured human subjects. Ann Surg. 258, 591–598 (2013). [PubMed: 23979273]
16. Qin C, Gu J, Hu J, et al. Platelets activation is associated with elevated plasma mitochondrial DNA during cardiopulmonary bypass. J Cardiothorac Surg. 11, 90–99 (2016). [PubMed: 27266529]
17. Corps KN, Roth TL, McGavern DB. Inflammation and neuroprotection in traumatic brain injury. JAMA Neurol. 72, 355–362 (2015). [PubMed: 25599342]
18. Zhang Q, Raoof M, Chen Y, et al. Circulating mitochondrial DAMPs cause inflammatory responses to injury. Nature. 464, 104–107 (2010). [PubMed: 20203610]
19. Maeda A, Fadeel B. Mitochondria released by cells undergoing TNF-α-induced necroptosis act as danger signals. Cell Death and Disease. 5, e1312; doi:10.138/cddis.2014.277 (2014). [PubMed: 24991764]
20. Boudreau LH, Duchez AC, Cloutier N, et al. Platelets release mitochondria serving as substrate for bactericidal group IIA-secreted phospholipase A2 to promote inflammation. Blood. 124, 2173–2183 (2014). [PubMed: 25082876]
21. West AP, Khoury-Hanold W, Staron M, et al. Mitochondrial DNA stress primes the antiviral innate immune response. Nature. 520, 553–557 (2015). [PubMed: 25642965]
22. Powels SD, Heijink IH, ten Hacken NHT, et al. DAMPs activating innate and adaptive immune responses in COPD. Mucosal Immunology. 7, 215–226 (2014). [PubMed: 24150257]

23. Braza F, Brouard S, Chadban S, Goldstein DR. Role of TLRs and DAMPs in allograft inflammation and transplant outcomes. Nat Rev Nephrol. 12, 281–290 (2016). [PubMed: 27026348]
24. Lin L, Xu H, Bishawi M, et al. Circulating mitochondria in organ donors promote allograft rejection. Am J Transplant. 19, 1917–1929 (2019). [PubMed: 30761731]
25. Oeckinghaus A, Hayden MS, Ghosh S. Crosstalk in NF-κB signaling pathways. Nat Immunol. 12, 695–708 (2011). [PubMed: 21772278]
26. Kempe S, Kestler H, Lasar A, Wirth T. NF-kB controls the global proinflammatory response in endothelial cells: evidence for the regulation of a pro-atherogenic program. Nucleic Acids Res. 33, 5308–5319 (2005). [PubMed: 16177180]
27. Ishikawa H, Ma Z, Barber GN. STING regulates intracellular DNA-mediated type I interferon-dependent innate immunity. Nature. 461, 788–892 (2009). [PubMed: 19776740]
28. Sun L, Wu J, Du F, Chen X, Chen ZJ. Cyclic GMP-AMP synthase is a cytosolic DNA sensor that activates the type I interferon pathway. Science. 339, 786–791 (2013). [PubMed: 23258413]
29. Abe T, Barber GN. Cytosolic-DNA-mediated, STING-dependent proinflammatory gene induction necessitates canonical NF-κB activation through TBK1. J Virol. 88, 5328–5341 (2014). [PubMed: 24600004]
30. Dunphy G, Flannery SM, Almine JF, et al. Non-canonical activation of the DNA sensing adaptor STING by ATM and IFI16 mediates NF-κB signaling after nuclear DNA damage. Mol Cell. 71, 745–760 (2018). [PubMed: 30193098]
31. Sallusto F, Lenig D, Forster R, Lipp M, Lanzavecchia A. Two subsets of memory T lymphocytes with distinct homing potentials and effector functions. Nature. 401, 708–712 (1999). [PubMed: 10537110]
32. Xu H, Perez S, Cheeseman A, Mehta AK, Kirk AD. The allo- and viral-specific immunosuppressive effect of belatacept, but not tacrolimus, attenuates with progressive T cell maturation. Am J Transplant. 14, 319–332 (2014). [PubMed: 24472192]
33. Read MA, Whitley MZ, Williams AJ, Collins T. NF-gB and Ir~B~: An Inducible Regulatory System in Endothelial Activation. J Exp Med. 179, 503–512 (1994). [PubMed: 7507507]
34. Collins T, Read MA, Neishi AS, Whitley MZ, Thanos D, Maniatis T. Transcriptional regulation of endothelial cell adhesion molecules: NF-kappa B and Cytokine-inducible enhancers. FASEB J. 9, 899–909 (1995). [PubMed: 7542214]
35. Smith J STING, the endoplasmic reticulum and mitochondria: is three a crowed or a conversation. Front Immunol. 10.3389/fimmu.2020, 61347 (2021).
36. Demaria O, Gassart AD, Coso S, et al. STING activation of tumor endothelial cells initiates spontaneous and therapeutic antitumor immunity. Proc Natl Acad Sci USA. 112, 15408–15413 (2015). [PubMed: 26607445]
37. Corrales L, Glickman LH, Dubensky TW Jr, Gajewski TF. Direct activation of STING in the tumor microenvironment leads to potent and systemic tumor regression and immunity. Cell Reports. 11, 1018–1030 (2015). [PubMed: 25959818]
38. Haag SM, Gulen MF, Reymond L, et al. Targeting STING with covalent small-molecule inhibitors. Nature. 559, 269–273 (2018). [PubMed: 29973723]
39. Zhou W, Whiteley AT, de Oliveira Mann CC, et al. Structure of human cGAS-DNA complex reveals enhanced control of immune surveillance. Cell. 174, 300–311 (2018). [PubMed: 30007416]
40. Unterholzner L, Keating SE, Baran M, et al. IFI16 is an innate immune sensor for intracellular DNA. Nat Immunol. 11, 997–1005 (2010). [PubMed: 20890285]
41. Gursel I, Gursel M, Yamada H, Ishil KJ, Takeshita F, Klinman DM. Repetitive elements in mammalian telomeres suppress bacterial DNA-induced immune activation. J Immunol. 171, 1393–1340 (2003). [PubMed: 12874230]
42. Kaminski JJ, Schattgen SA, Tzeng TC, Bode C, Klinman DM, Fitzgerald KA. Synthetic oligodeoxynucleotides containing suppressive TTAGGG motifs inhibits AIM2 inflammasome activation. J Immunol. 191, 3876–3883 (2013). [PubMed: 23986531]
43. Pegu A, Qin S, Fallert BA, Nisato RE, Peper MS, Reinhart TA. Human lymphatic endothelial cells express multiple functional TLRs. J Immunol. 180, 3399–3405 (2008). [PubMed: 18292566]

44. Kebir DE, Jozsef L, Pan W, Wang L, Filep JG. Bacterial DNA activates endothelial cells and promotes neutrophil adherence through TLR9 signaling. J Immunol. 182:4386–4394 (2009). [PubMed: 19299739]
45. Takeda K, Akira S. TLR signaling pathways. Seminars in Immunol. 16:3–9 (2004).
46. Ramirez-Ortiz ZG. Pendergraft WF, Prasad A, et al. The scavenger receptor SCARF1 mediated the clearance of apoptotic cells and prevents autoimmunity. Nat Immunol. 14:917–926 (2013). [PubMed: 23892722]
47. Happonen KE, Tran S, Morgelin M, et al. The gas6-axl protein interaction mediates endothelial uptake of platelet microparticles. J Biol Chem. 291:10586–10601 (2016). [PubMed: 27006397]
48. Liu D, Wu H, Wang C, Li Y, Tian H, Siraj S, et al. STING directly activates autophagy to turn the innate immune response. Cell Death Differ. 26:17352–1749 (2019).
49. Gui X, Yang H, Li T, Tan X, Shi P, Li M, Du F, Chen Z. Autophagy induction via STING trafficking is primordial function of the cGAS pathway. Nature. 567:262–266 (2019). [PubMed: 30842662]
50. Pickrell AM, Youle RJ. The roles of PINK1, parkin, and mitochondrial fidelity in Parkinson's disease. Neuron. 85:257–273 (2015). [PubMed: 25611507]
51. Sliter DA, Martinex J, Hao L, Chen X, Sun N, Fischer TD, et al. Parkin and PINK1 mitigate STING-induced inflammation. Nature. 561:258–262 (2018). [PubMed: 30135585]
52. Pollara J, Edward RW, Lin L, Bendersky VA, Brennan T. Circulating mitochondria in deceased organ donors are associated with immune activation and early allograft dysfunction. J Clin Invest insight jci.insight.121622 (2018).
53. Auphan N, DiDonato JA, Rosette C, Helmberg A, Karin M. Immunosuppression by glucocorticoids: inhibition of NF-kB activity through induction of IkB synthesis. Science. 270:286–290 (1995). [PubMed: 7569976]
54. Morgan MJ, Liu ZG. Crosstalk of reactive oxygen species and NF-κB signaling. Cell Research. 21:103–115 (2011). [PubMed: 21187859]
55. Leifer CA, Medvedev AE. Molecular mechanisms of regulation of Toll-like receptor signaling. J Leukoc Biol. 100:927–941 (2016). [PubMed: 27343013]
56. Tait SWG, Green DR. Mitochondria and cell death: outer membrane permeabilization and beyond. Nat Rev Mol Cell Biol. 11:621–632 (2010). [PubMed: 20683470]
57. Tondera D, Grandemange S, Jourdain A, et al. SLP-2 is required for stress-induced mitochondrial hyperfusion. EMBO J. 28:1589–1600 (2009). [PubMed: 19360003]
58. Westermann B Mitochondrial fusion and fission in cell life and death. Nat Rev Mol Cell Biol. 11:872–884 (2010). [PubMed: 21102612]
59. Youle RJ, van der Bliek AM. Mitochondrial fission, fusion, and stress. Science. 337:1062–1065 (2012). [PubMed: 22936770]
60. Yorimitsu T, Klionsky DJ. Autophagy: molecular machinery for self-eating. Cell Death Differ. 12:1542–1552 (2005). [PubMed: 16247502]
61. Lo D, Weaver TA, Stempora L, et al. Selective targeting of human alloresponsive CD8+ effector memory T cells based on CD2 expression. Am J Transplant. 11:22–33 (2011). [PubMed: 21070604]
62. Schmitz R, Fitch ZW, Xu H, Ghali A, Mehta AK, Guasch A, Kirk A. Kidney transplantation using alemtuzumab, belatacept, and sirolimus: five-year follow-up. Am J Transplant. 20:3609–3619 (2020). [PubMed: 32515087]
63. Adams AB, Goldstein J, Garrett C, et al. Belatacept combined with transient calcineurin inhibitor therapy prevents rejection and promotes improved long-term renal allograft function. Am J Transplant. 17:2922–2936 (2017). [PubMed: 28544101]
64. Jassem W, Heaton ND. The role of mitochondria in ischemia/reperfusion injury in organ transplantation. Kidney Int. 66:514–517 (2004). [PubMed: 15253700]
65. Weiss S, Kotsch K, Francuski M, et al. Brain death activates donor organs and is associated with a worse I/R injury after liver transplantation. Am J Transplant. 7:1584–1593 (2007). [PubMed: 17430397]

66. Wilhelm MJ, Pratschke J, Beato F, et al. Activation of the heart by donor brain death accelerates acute rejection after transplantation. Circulation. 102:2426–2433 (2000). [PubMed: 11067799]

67. Kruger B, Krick S, Dhillon N, et al. Donor toll-like receptor 4 contributes to ischemia and reperfusion injury following human kidney transplantation. Proc Natl Acad Sci USA. 106:3390–3395 (2009). [PubMed: 19218437]

a

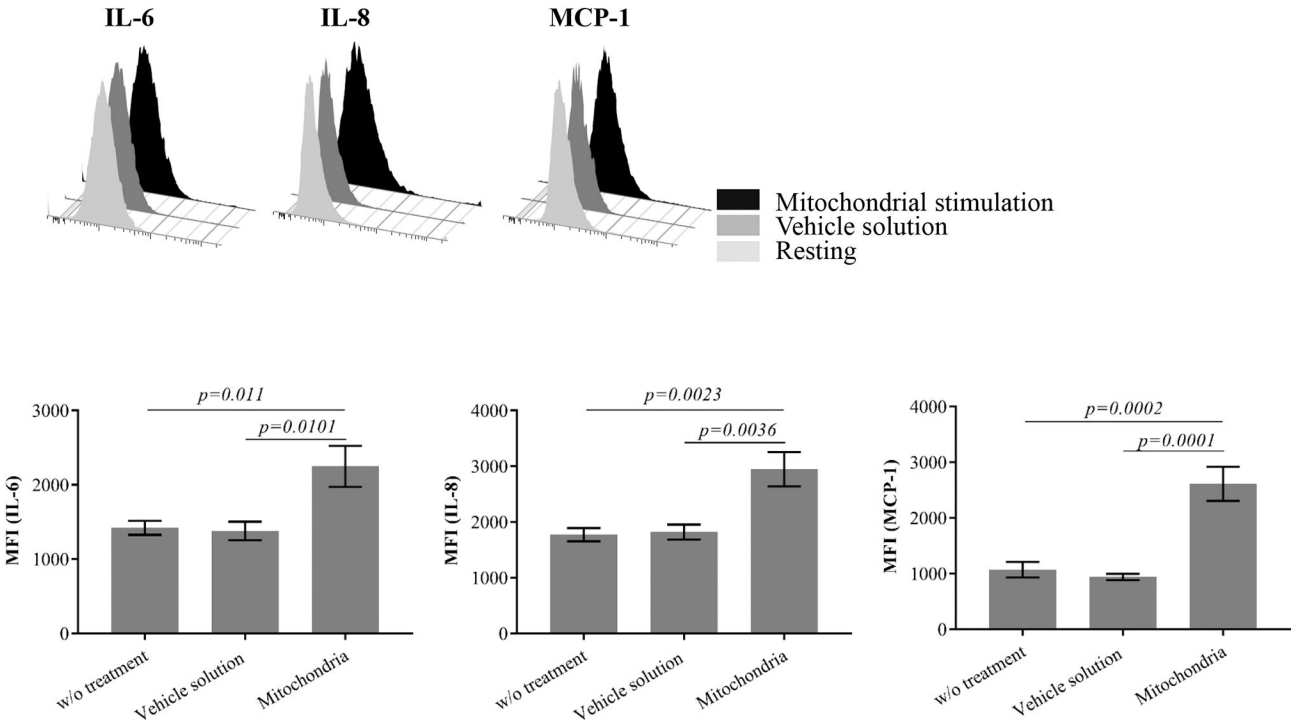

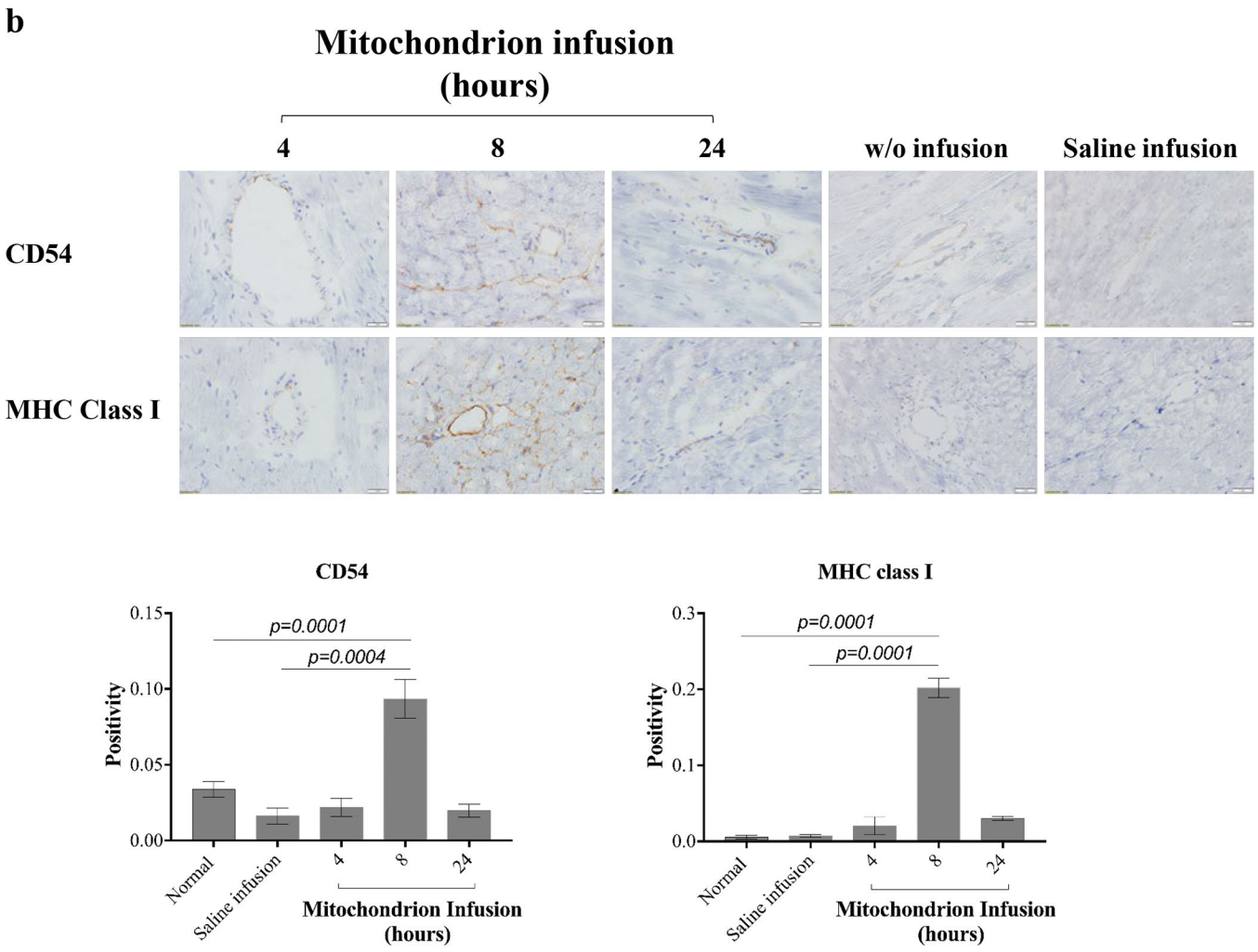

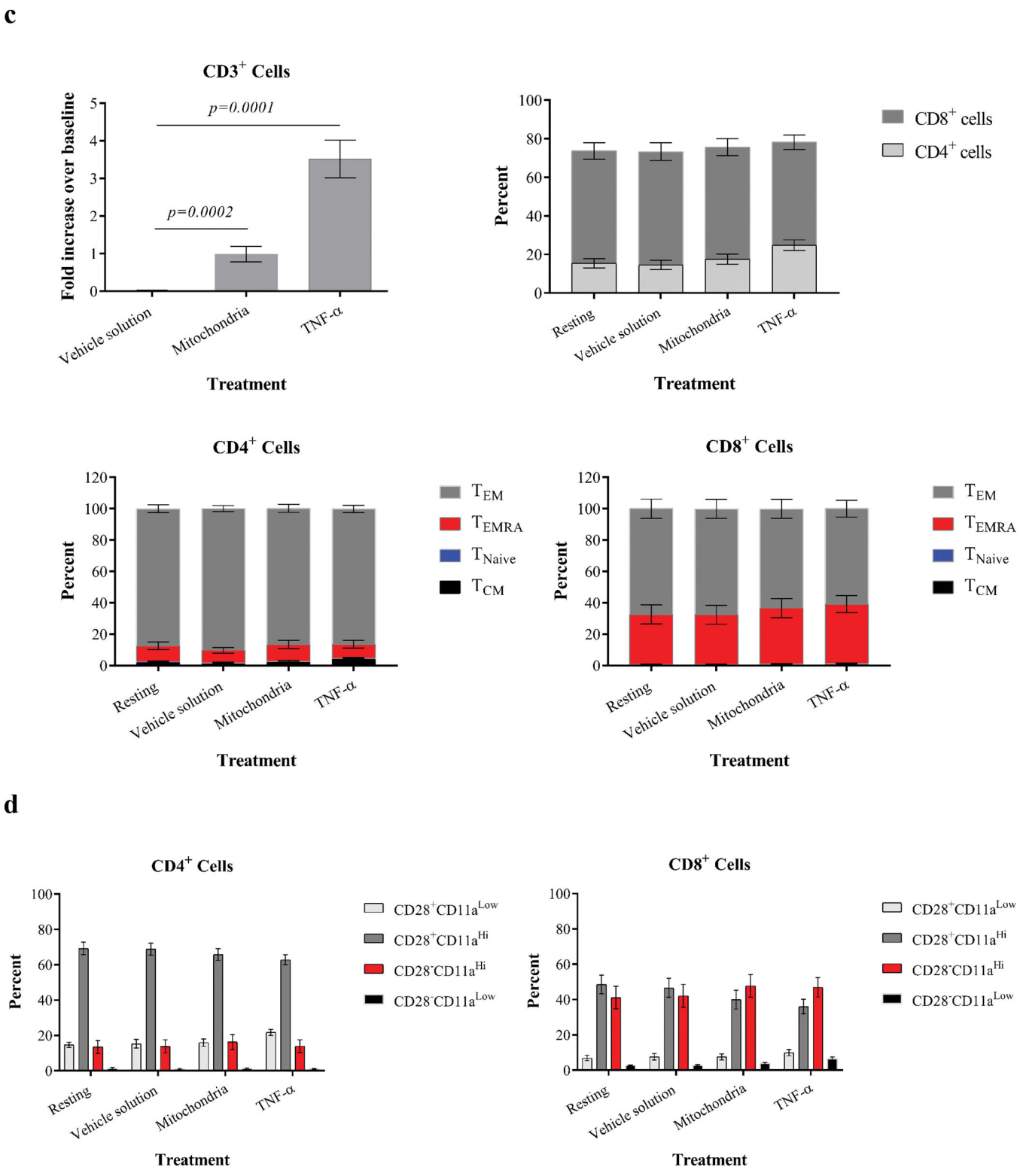

Figure 1. Exogenous mitochondria activate aortic endothelial cells and augment allospecific T cell responses.

(a) The production of IL-6, IL-8, and MCP-1 is detected by intracellular cytokine staining. A representative experiment is shown as histogram demonstrating upregulation of cytokines following mitochondrial stimulation (black) when compared with vehicle solution (dark gray) and unstimulated (light gray) cells. Mitochondrion–stimulated ECs show upregulation of cytokine expression (bottom panel). (b) Evaluation of CD54 and MHC class-I expression on mouse heart ECs post-mitochondria infusion. Normal saline perfusion shows minimal CD54 and MHC class-I expression on cardiac ECs. Semi-quantitative analysis shows increased CD54 and MHC class-I expression on cardiac ECs at 8 hours post-mitochondrial infusion. (c) Untreated ECs and ECs, pretreated with purified mitochondria, vehicle solution, or TNF-α (positive controls), are co-incubated with human PBMCs for 2 hours. The adherent T cells were stained and analyzed by FACS. T cells are segregated by gating on $CD3^+CD14^-$ cells, followed by gating on $CD4^+$ and $CD8^+$ subsets, and the phenotype of cells subsequently analyzed based on CCR7/CD45RA and CD11a/CD28 expression. 12-hour treatment of ECs with exogenous mitochondria leads to a significant increase in $CD3^+$ cells adherent. The majority of adherent $CD3^+$ cells are $CD8^+$ cells, and the adherent $CD3^+CD4^+$ and $CD3^+CD8^+$ cells are predominantly T_{EM} and T_{EMRA} cells. (d) The adherent $CD4^+$ and $CD8^+$ cells highly express CD11a, and a large fraction of $CD8^+$ cells lacks CD28 expression. All experiments are repeated at least three times. The mean ± SD (standard deviation) is shown in all graphs.

a

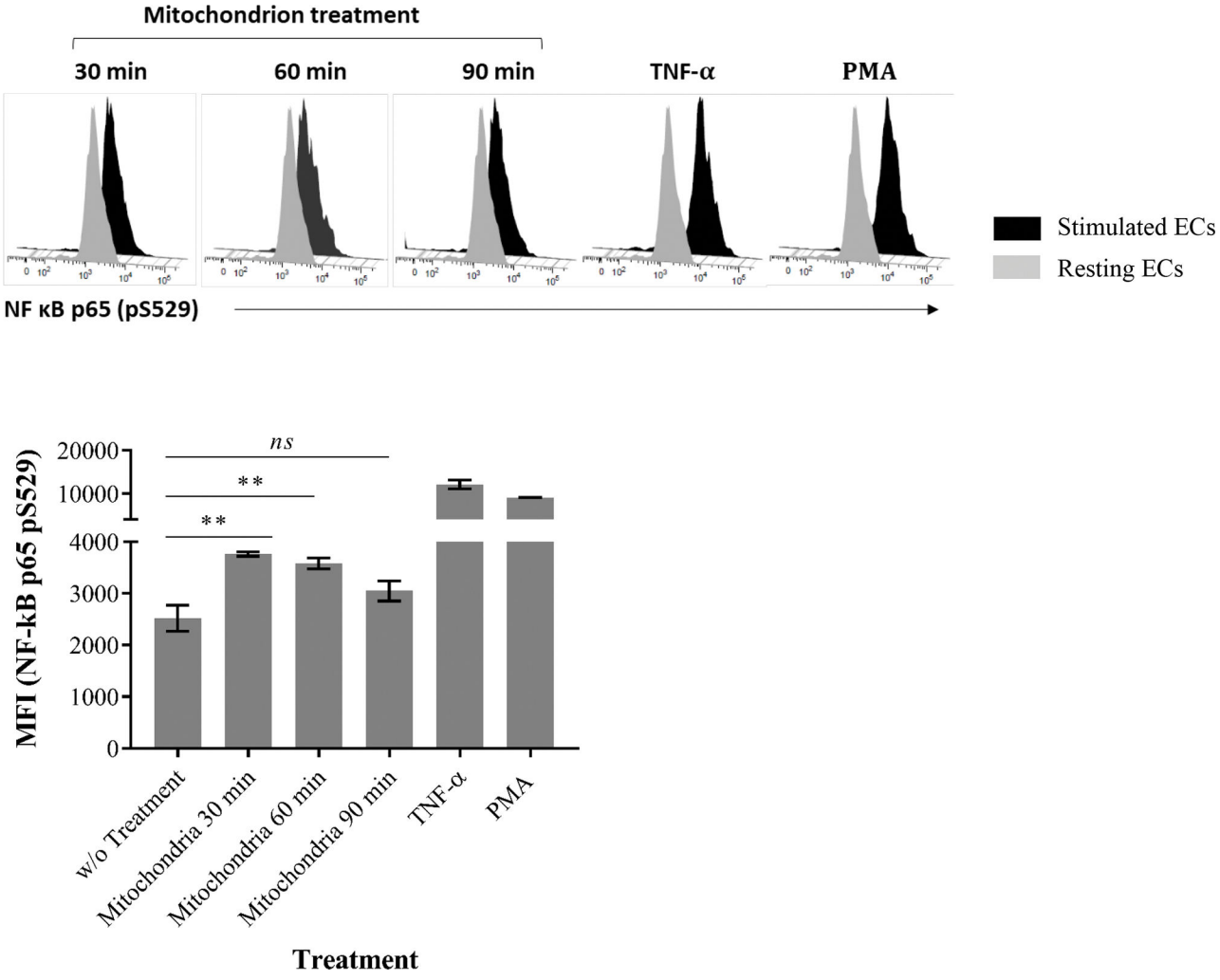

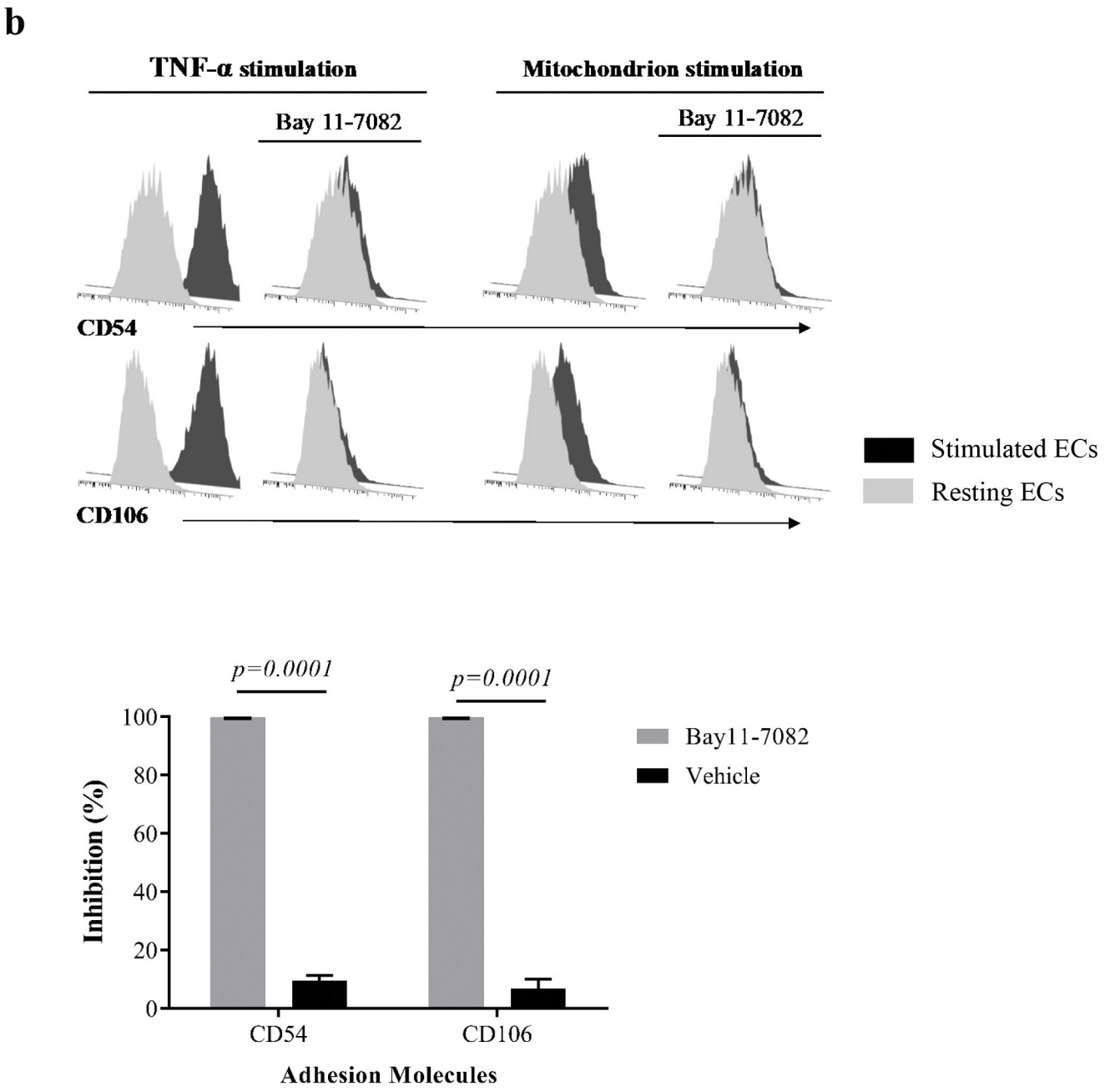

Figure 2. Phosphorylation of endothelial NF-κB p65 at serine residue 529 following stimulation by mitochondria.

(a) A representative experiment (top panel) shows increased NF-κB p65 phosphorylation at serine residue 529 following stimulation by exogenous mitochondria, TNF-α, and PMA. Unstimulated ECs is used as negative control. The bottom panel shows significant phosphorylation of NF-κB p65 phosphorylation at serine 529 (pS529) when compared with untreated ECs (**$p<0.001$). (b) A representative experiment is shown in the top panel demonstrating effectiveness of NF-κB inhibitor in preventing EC activation after stimulation by mitochondria or TNF-α, a positive control. Bay 11–7082 but not vehicle solution

completely prevent mitochondrion-induced EC activation (bottom). All experiments were repeated at least three times, and the mean ± SD is shown in graphs.

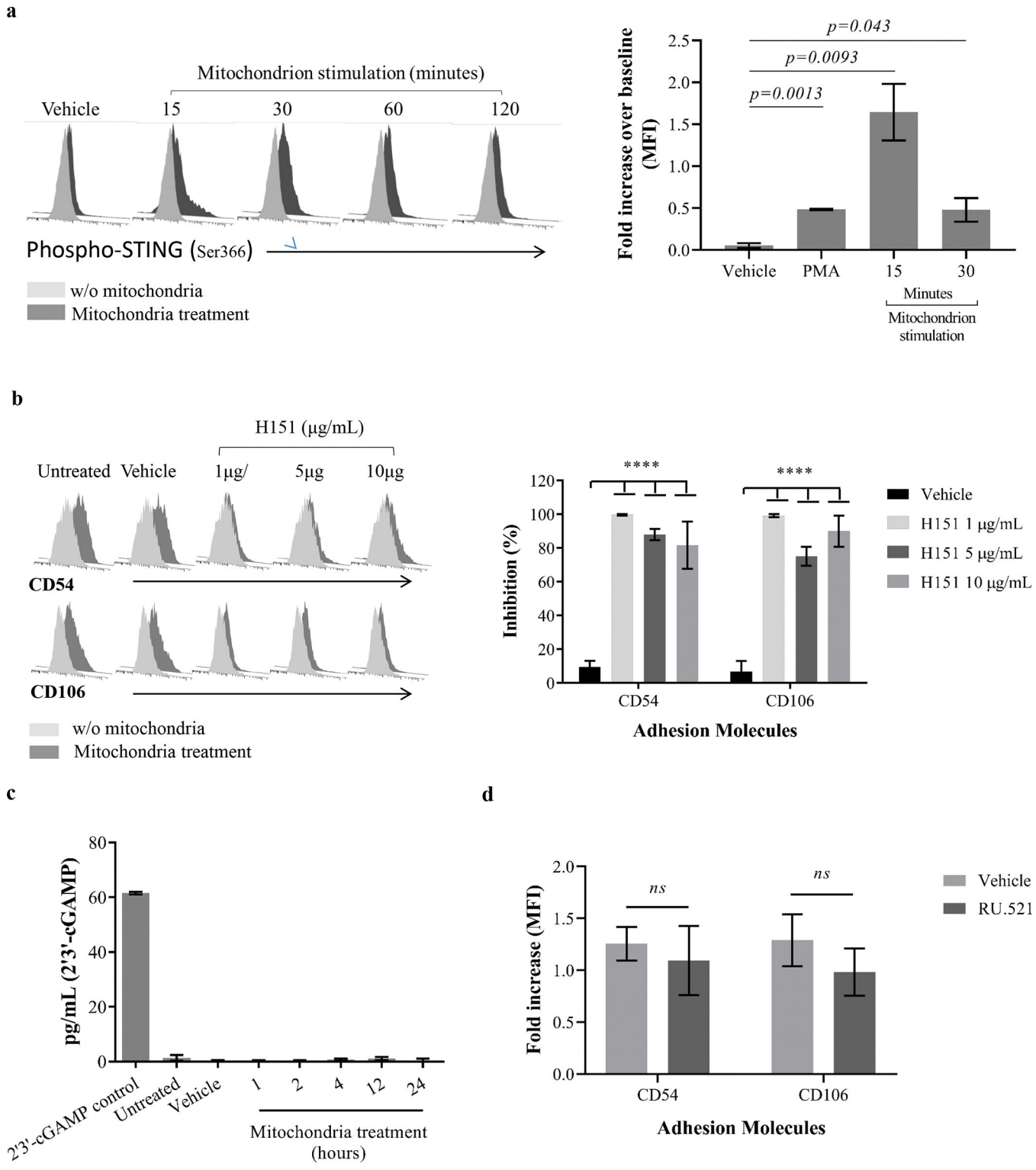

Figure 3. Evaluation of endothelial STING signaling following mitochondrion-induced EC activation.

(a) A representative experiment (top panel) shows STING activation as determined by phosphorylation at site Ser366, measured by FACS after mitochondrial stimulation. STING

phosphorylation increases significantly at 15 minutes post–mitochondrial stimulation, as expressed by fold increase of MFI over baseline when compared with vehicle solution treatment. (b) STING specific inhibitor H151 significantly inhibits mitochondria-induced EC activation (****$p<0.00001$). (c) ELISA barely detects 2′3′cGAMP in mitochondrion–stimulated ECs, a second messenger generated by cGAS. (d) The inhibition of cGAS by RU.521 fails to prevent mitochondrion–induced EC activation. All experiments were repeated at least three times, and the mean ± SD is shown in graphs.

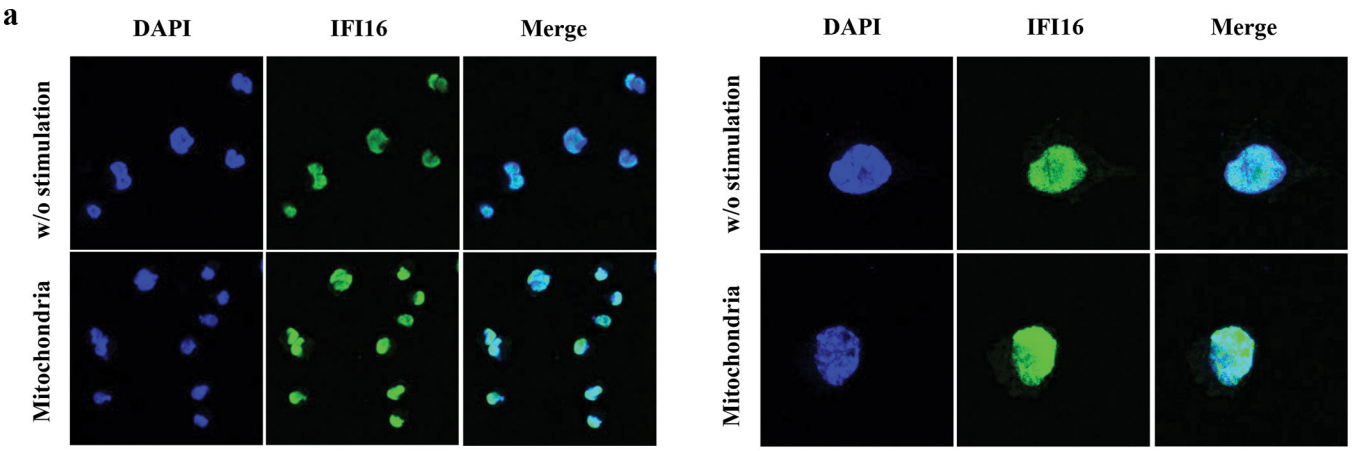

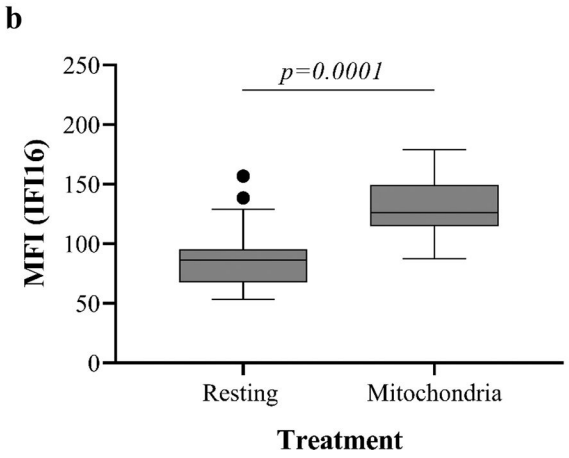

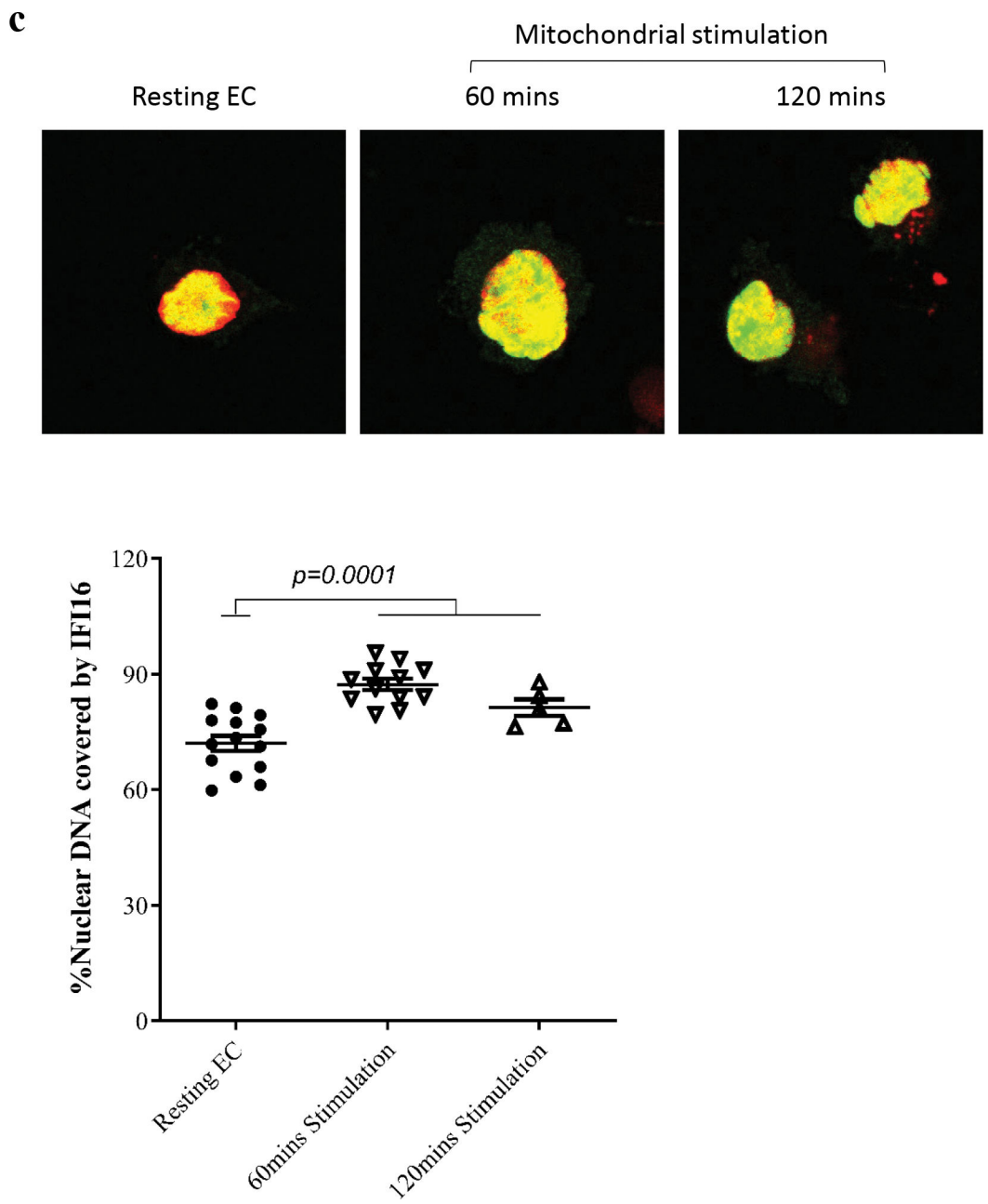

d

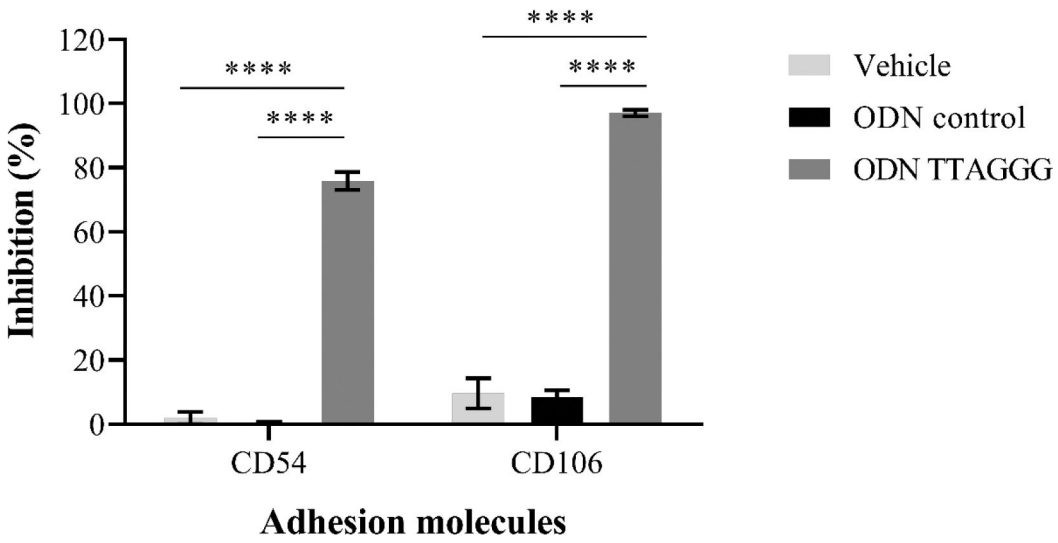

Figure 4. IFI16 expression in ECs following exogenous mitochondria stimulation.

(a) The florescent microscopic images of ECs following stimulation by mitochondria demonstrate increased IFI16 expression when compared with unstimulated ECs. The images on left show intracellular IFI16 expression (green) determined by a Plan-Apochromat oil lens (63X/1.00). The nuclear DNA was stained with DAPI (blue), and the images on the right were analyzed by oil lens at 63X/3.00 demonstrating the localization and distribution of IFI16 within EC nuclei, with or without mitochondrial stimulation. (b) The MFI of single cells was analyzed and measured by Fiji ImageJ software. Mitochondrion-stimulated cells (n=38) had a significantly higher MFI than resting ECs (n=28), as analyzed by two-tailed *t* test. (c) Representative confocal images illustrating correlation of intracellular IFI16 expression (green) with nuclear DNA (red) in ECs with or without mitochondrial stimulation (63X/3.00). The overlap (yellow) represents the binding of IFI16 with nuclear DNA. Nuclear DNA covered by IFI16 protein increases significantly (bottom panel) with an increase in free IFI16 as determined by one-way ANOVA (Kruskal-Wallis test) analysis. (d) Inhibition of IFI16 with ODN TTAGGG, but not ODN control, dramatically prevents EC activation after incubation with mitochondria (****$p<0.00001$). All experiments were repeated at least three times, and the mean ± SD is shown in graphs.

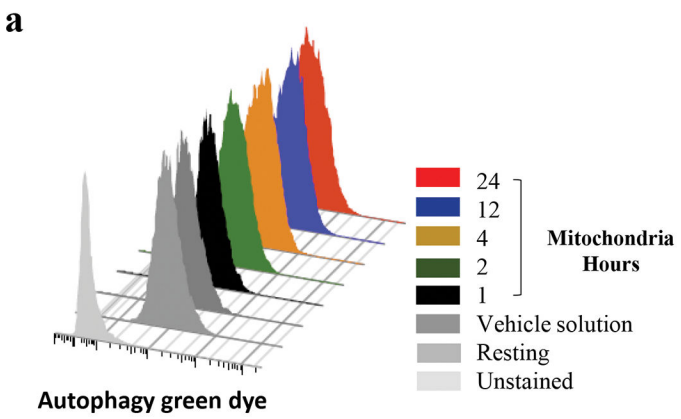

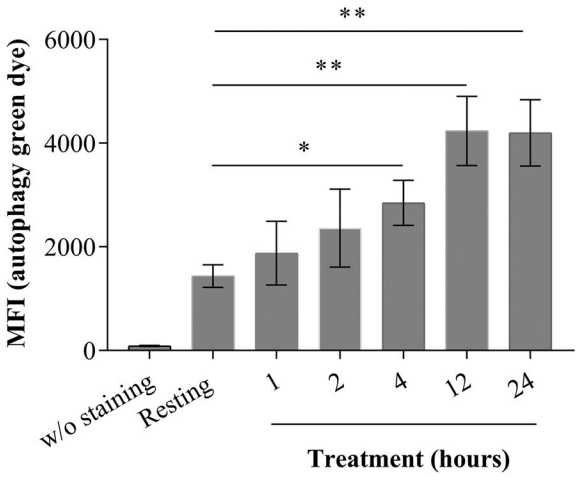

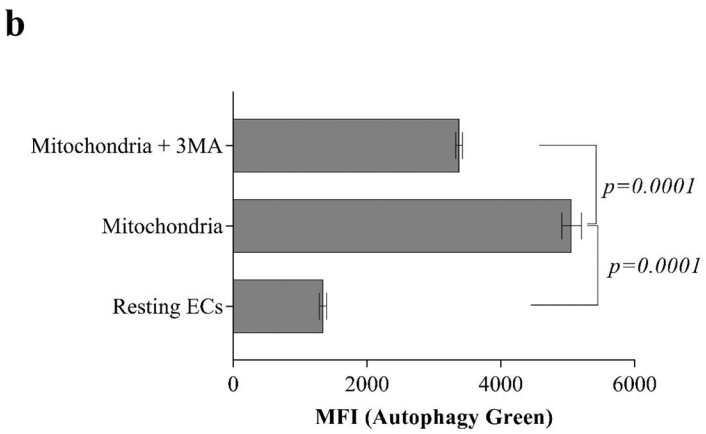

c

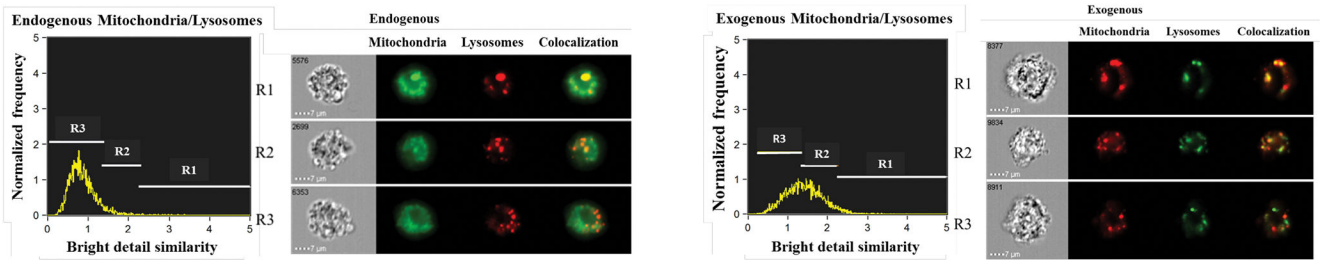

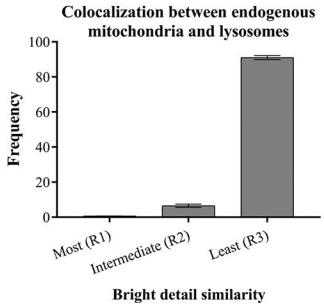

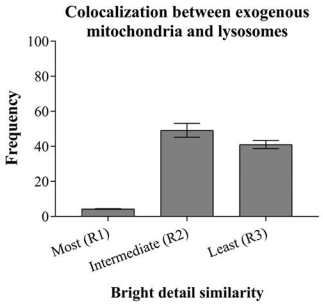

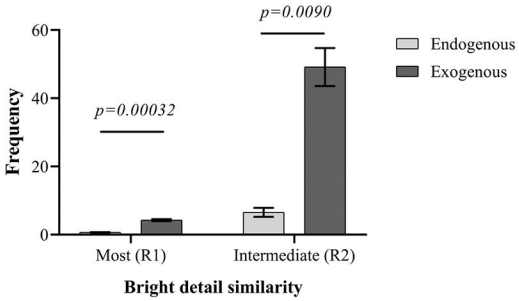

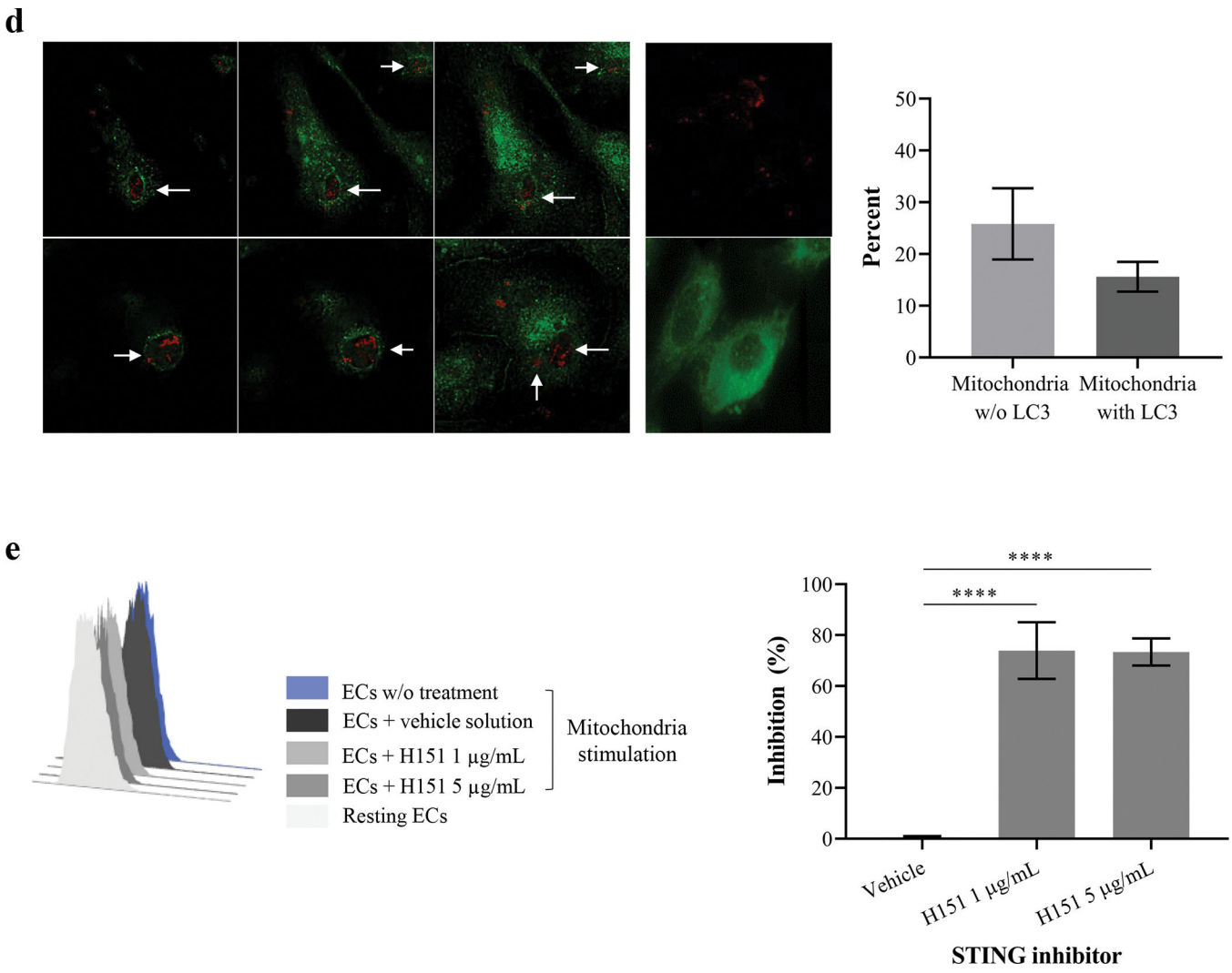

Figure 5. Increasing mitophagy activity in ECs following internalization of exogenous mitochondria.

(a) A representative experiment shows increasing mitophagy in mitochondrion–stimulated ECs stained with autophagic green dye (left). Exogenous mitochondrial stimulation significantly induced autophagy in ECs when compared with untreated ECs (right). (b) Inhibition of autophagy with 3-MA, an inhibitor specific for type-III phosphatidylinositol 3-kinases, partially reduced autophagy in mitochondrion-stimulated ECs. (c) ECs were pre-labeled with MitoTracker-Green and LysoTracker-Blue, and then incubated with dsRed-expressing exogenous mitochondria followed by acquisition of at least 5000 cells with ImageStream®^{X} Mark II Imaging FACS. The colocalization is determined by bright detail similarity after the merger of LysoTracker with MitoTracker or dsRed channels. The top left shows a representative experimental analysis of colocalization of endothelial lysosome (red) with endogenous mitochondria (green). A representative experiment demonstrating colocalization of exogenous mitochondria (red) with endothelial lysosome (green) is showed on the top right left. The colocalization of endogenous mitochondria with lysosome was minimally detectable (bottom left). In contrast, a dramatic increased colocalization

of exogenous mitochondria with lysosome was observed (bottom middle), and the colocalization of lysosome with exogenous mitochondria is significantly higher than with endogenous mitochondria (bottom right). (d) Representative confocal images illustrating mitophagosome formation induced by exogenous mitochondria intake. dsRed-expressing mitochondria are incubated with ECs for 12 hours and stained with anti-LC3 (in green) antibody. 3-D images were collected with 0.25um increments by Zeiss LSM 780 Axio Examiner with a Plan-Apochromat (63X/1.40) oil lens. Selective optical sections from top to bottom were included to illustrate autophagosomes formed at different depth within ECs (white arrow). ECs, stained with secondary but not anti-LC3 primary antibody, were negative controls (top right). Untreated ECs were minimally stained with LC3 without formation of autophagosomes (bottom right). The autophagosomes in ECs (n=40) following internalization of dsRed expressing mitochondria are semi-quantified (right). (e) To determine the role of STING in mitochondrion-induced mitophagy, ECs, pre-treated with H115, are incubated with purified mitochondria, and stained with autophagy greed dye. A representative experiment is shown on left demonstrating reduction of mitophagy in ECs treated with STING inhibitor. The inhibition of STING activation is effective to prevent mitochondrion–induced mitophagy in ECs (right). All experiments were repeated at least three times, and the mean ± SD is shown in graphs. (*$p<0.05$, **$p<0.001$, ****$p<0.00001$)